Bioorganic & Medicinal Chemistry 19 (2011) 3884–3891

Contents lists available at ScienceDirect

Bioorganic & Medicinal Chemistry

journal homepage: www.elsevier.com/locate/bmc

4-Alkoxy-3-arylfuran-2(5*H*)-ones as inhibitors of tyrosyl-tRNA synthetase: Synthesis, molecular docking and antibacterial evaluation

Zhu-Ping Xiao [a,b,*], Hui Ouyang [a], Xu-Dong Wang [a], Peng-Cheng Lv [b], Ze-Jun Huang [a], She-Rong Yu [a], Tian-Fang Yi [a], Ye-Ling Yang [a], Hai-Liang Zhu [a,b,*]

[a] College of Chemistry & Chemical Engineering, and Key Laboratory of Hunan Forest Products and Chemical Industry Engineering, Jishou University, Jishou 416000, PR China
[b] State Key Laboratory of Pharmaceutical Biotechnology, Nanjing University, Nanjing 210093, PR China

ARTICLE INFO

Article history:
Received 20 April 2011
Revised 22 May 2011
Accepted 23 May 2011
Available online 27 May 2011

Keywords:
Furanone
Antibacterial
Tyrosyl-tRNA synthetase
Structure–activity relationship
Molecular docking

ABSTRACT

A series of novel 4-alkoxy-3-arylfuran-2(5*H*)-ones as tyrosyl-tRNA synthetase inhibitors were synthesized. Of these compounds, 3-(4-hydroxyphenyl)-4-(2-morpholinoethoxy)furan-2(5*H*)-one (**27**) was the most potent. The binding model and structure–activity relationship indicate that replacement of morpholine-ring in the side chain of **27** with a substituent containing more hydrophilic groups would be more suitable for further modification. Antibacterial assay revealed that the synthetic compounds are effective against growth of Gram-positive organisms, and **27** is the most potent agent against *Staphylococcus aureus* ATCC 25923 with MIC_{50} value of 0.23 μg/mL.

1. Introduction

Aminoacyl-tRNA synthetases (aaRSs) are the enzymes that catalyze the transfer of amino acids to their cognate tRNAs,[1,2] and their catalytic activities determine the genetic code. For this reason, these enzymes are essential for protein synthesis and cell viability,[3,4] and they are potential targets for antibacterial agents.[5,3,6] This concept is proven by the success of the broad-spectrum antibacterial drug mupirocin, which targets bacterial isoleucyl-tRNA synthetases (IleRS).[7] Additionally, AN-2690 (Scheme 1), an inhibitor of leucyl-tRNA synthetases, is currently in clinical development for the topical treatment of onychomycosis and icofungipen (Scheme 1), another inhibitor of IleRS, reached clinical phase II for the systemic treatment of oropharyngeal candidiasis.[8]

Many compounds with γ-butyrolactone-core (furanone) show diverse biological activities such as antitumor and anti-inflammatory activity.[9–12] It is reported that butalactin (Scheme 1) exhibits moderate antibacterial activity against Gram-positive bacteria.[13] Based on this findings, Lattmann et al. reported some derivatives of γ-butyrolactone (5-alkoxy-4-aminofuran-2(5*H*)-one, Scheme 1) showing good antibacterial activity against multiresistant *Staphylococcus aureus*.[14] In our work for finding new antibacterial agents,[15,16] we have shown that 3-aryl-4-alkylaminofuran-2(5*H*)-ones are potent inhibitors against tyrosyl-tRNA synthetase (TyrRS),[17] one of the aminoacyl-tRNA synthetases (aaRSs). Structure–activity relationships of this class of compounds disclosed that separation of amino moiety and furanone fragment with an aminoethylene group spacer led to compound (**4** vs **5**, Scheme 1) being more potent. Compound **5** (with IC_{50} of 3.3 μM against TyrRS) was therefore used as lead compound for further modification, and two strategies for side-chain modification were used at the first stage. One is replacement of morpholine ring with other heterocycles and the other is replacement of NH group with O atom. Several compounds were then synthesized for determining their inhibitory activities against TyrRS. The results disclosed that bioisosteric replacement of NH group (**5**) with an O (**24**, Scheme 1) was more favorable for activity. In this context, we would like to report synthesis of 4-alkoxy-3-arylfuran-2(5*H*)-ones and their determination as TyrRS inhibitors and antibacterials. The results disclose some of the synthesized compounds exhibited very good antibacterial activities.

2. Results and discussion

2.1. Chemistry

Twenty-two 4-alkoxy-3-arylfuran-2(5*H*)-ones were designed and synthesized by the routes outlined in Scheme 2 and Scheme 3. 3-Aryl-4-(2-bromoethoxy)furan-2(5*H*)-ones, **3**, were prepared

* Corresponding authors. Tel.: +86 743 8563911; fax: +86 743 8563911 (Z.-P.X.); tel.: +86 25 83592572; fax: +86 25 83592672 (H.-L.Z.).
E-mail addresses: xiaozhuping2005@163.com (Z.-P. Xiao), zhuhl@nju.edu.cn (H.-L. Zhu).

0968-0896/$ - see front matter © 2011 Elsevier Ltd. All rights reserved.
doi:10.1016/j.bmc.2011.05.042

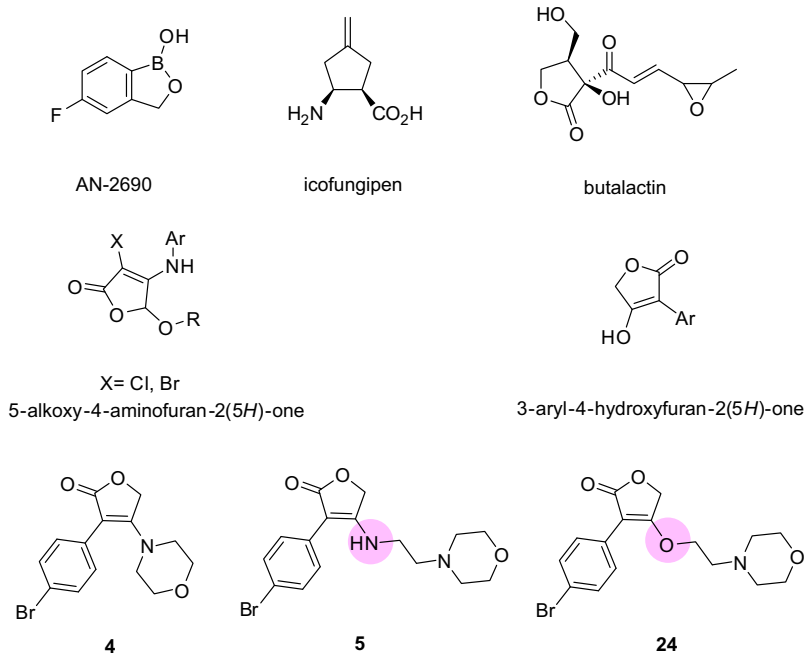

Scheme 1. Structures of some compounds and the evolution process of 4-alkoxy-3-arylfuran-2(5*H*)-one.

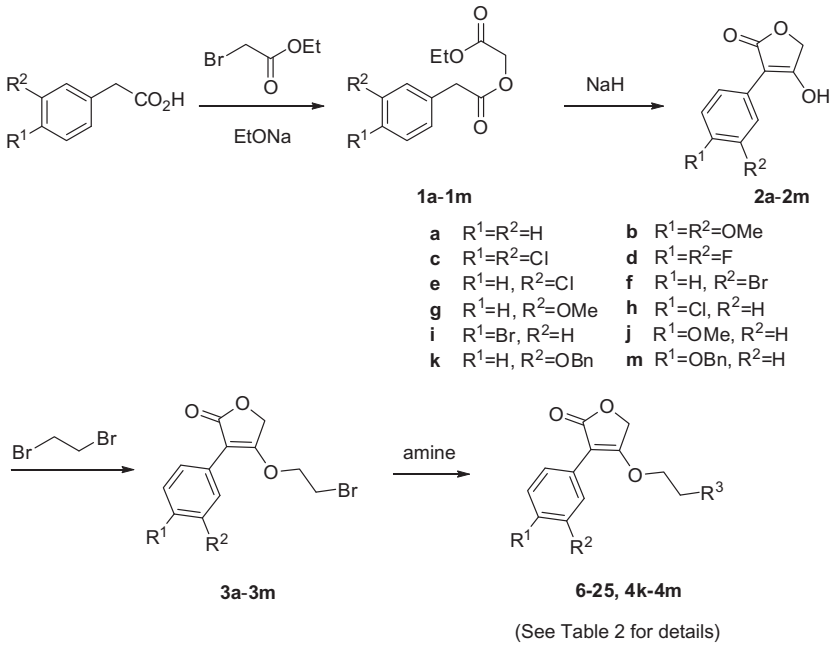

Scheme 2. Synthetic route of 4-alkoxy-3-arylfuran-2(5*H*)-ones.

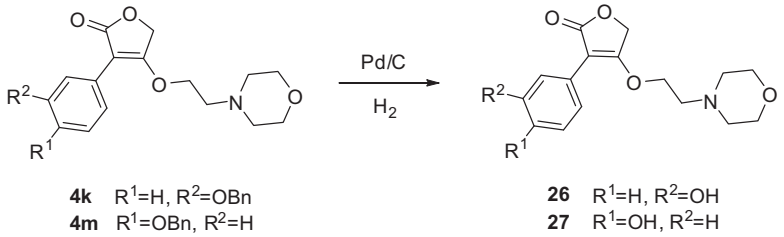

Scheme 3. The synthesis of **26** and **27**.

from the corresponding 3-aryl-4-hydroxyfuran-2(5*H*)-ones (**2**) which were synthesized according to the previously reported method with some modifications.[9] In brief, esters **1** were formed by the condensation of an appropriately substituted phenylacetic acid with ethyl bromoacetate in the presence of sodium ethoxide. Compounds **2** were subsequently prepared via alkaline cyclization of **1** using sodium hydride in dry THF. Displacement of a bromine in 1,2-dibromoethane with **2** was normally conducted in dry acetone in the presence of triethylamine. The desired amines (**6**–**25**) were obtained by amination of **3a**–**3j** with appropriate aliphatic amines in DMF in the presence of triethylamine. Compound **4k** and **4m** were similarly obtained by amination of **3k** and **3m**, followed by debenzylation over Pd/C under hydrogen atmosphere, to generate **26** and **27**. All 4-alkoxy-3-arylfuran-2(5*H*)-ones are the first reported and were fully characterized by spectroscopic methods and elemental analysis together with a crystal structure (**11**).

2.2. Description of the crystal structure

Compound **11** was determined by X-ray diffraction analysis (Fig. 1). The crystal data are presented in Table 1 and some important bond lengths were given in Table 2. The bond length of C7–C10 is 1.348(3) Å, following in the range of a typical C–C double bond.[18,19] Compound **11** was therefore identified as a furan-2(5*H*)-one not a furan-2(3*H*)-one. ^{1}H NMR spectrum of **11** provides another evidence for this assignment. For the furanone moiety, the ^{1}H NMR spectrum displayed the two proton signals as singlet at about δH 5.0. Comparisons ^{1}H NMR spectrum of **11** with others, all synthetic compounds were determined as furan-2(5*H*)-ones. Because C9 attaches to a double bond, σ–π hyperconjugation occurring between C9–H9A (H9B) and C7–C10 slightly shortens C9–C10 bond from about 1.53[20] to 1.489(3) Å. C10–O3 (1.326(2) Å) bond has shorter bond distance than the standard C–O single bond (1.43 Å),[16] but longer than C–O double bond (1.20 Å).[19] This clearly indicated that an sp^3 orbital of O3 is conjugated with the π molecular orbital of C7–C10 double bond, which was supported by the small torsion angle (0.6(8)°) of C8–C7–C10–O3.

The stereochemistry of the double bond in lactone ring was assigned as (*E*)-configuration based on X-ray crystallography of product **11** (Fig. 1). This gives a basis for assigning the *E* configuration to all newly synthetic 4-alkoxy-3-arylfuran-2(5*H*)-ones.

2.3. Inhibitory activities of 4-alkoxy-3-arylfuran-2(5*H*)-ones against TyrRS from *S. aureus*

All the synthesized compounds (**6**–**27**) were tested for inhibitory activity against TyrRS from *S. aureus*. The IC$_{50}$s of these compounds are presented in Table 3. Compounds **6**–**14** were prepared to study the utility of aliphatic side chains and compound **11** was proved as the most potent in this series, having IC$_{50}$ of 6.2 ± 0.9 μM. Replacement of *N*-morpholino group in the side chain of **11** with hydrophilic substituent (4-methylpiperazinyl group) shows similar potency. While compounds **6**–**10**, with an aliphatic amino group in the side chain, were less effective, and those with an aryl ring in the side chain (**13** and **14**) were inactive, indicating that a hydrophobic group in the side chain is detrimental. Therefore, this position seems to be more suitable for further modification with a substituent containing more hydrophilic groups.

We then turned our attention toward exploring the SAR profile of the phenyl group (**15**–**27**). The compound **27** with a hydroxyl group at the *para* position of the benzene-ring fragment exerted the highest inhibitory activity against *S. aureus* TyrRS with an

Table 1
Crystal structure data for compound **11**

Compound	**11**
Formula	$C_{16}H_{19}NO_4$
Mr	289.32
Crystal size/mm^3	0.20 × 0.20 × 0.10
Crystal system	Monoclinic
Space group	P 2$_1$/c
a/Å	8.4449(9)
b/Å	18.9619(19)
c/Å	9.4747(10)
β/°	100.279(2)
V/Å^3	1492.8(3)
Z	4
Dc/(g/cm^{-3})	1.287
μ/mm^{-1}	0.093
F(0 0 0)	616
Max. and min. trans.	0.9908 and 0.9817
θ range/°	2.15/28.29
Index range (*h*, *k*, *l*)	−6/11, −25/25, −12/12
Reflections collected/unique	11735/3689
Data/restraints/parameters	3689/0/190
R_{int}	0.0304
Goodness-of-fit on F^2	1.139
R_1, wR_2 [$I > 2\sigma(I)$]	0.0759/0.1002
R_1, wR_2	0.1814/0.1681
Extinction coefficient	–
$(\Delta\rho)_{max}$, $(\Delta\rho)_{min}$ (e/Å^3)	0.246/−0.228

Table 2
Important bond lengths (Å) of compound **11**

Bond	Bond length	Bond	Bond length
C1–C7	1.476(3)	C9–C10	1.489(3)
C7–C8	1.464(3)	C10–O3	1.326(2)
C7–C10	1.348(3)	C11–O3	1.446(2)

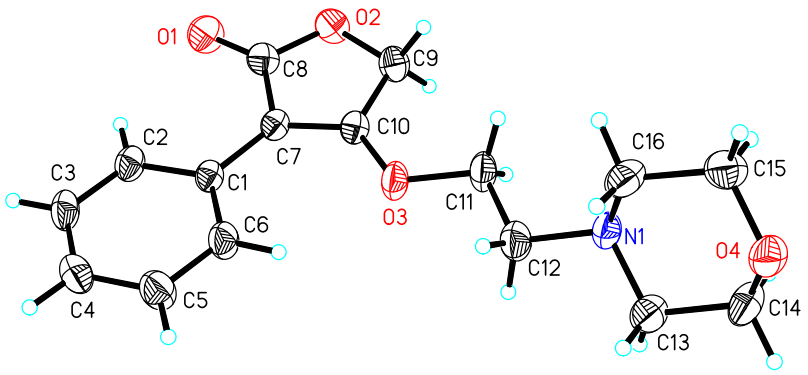

Figure 1. Molecular structure of compound **11**, showing the atom-numbering scheme. Displacement ellipsoids are drawn at the 30% probability level.

Table 3
In vitro inhibitory activity data of the synthesized compounds against *S. aureus* TyrRS

Compound	Structure			IC_{50} (μM)
	R^1	R^2	R^3	
6	H	H		29.1 ± 4.3
7	H	H	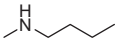	71.9 ± 15.6
8	H	H		87.4 ± 17.3
9	H	H		53.6 ± 10.9
10	H	H		35.5 ± 7.1
11	H	H		6.2 ± 0.9
12	H	H	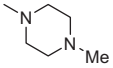	8.6 ± 1.2
13	H	H	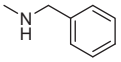	>100
14	H	H	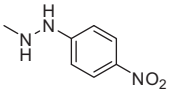	>100
15	OMe	OMe		>100
16	OMe	OMe		>100
17	OMe	OMe	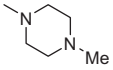	>100
18	Cl	Cl	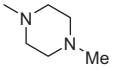	>100
19	F	F		>100
20	H	Cl		20.5 ± 4.8
21	H	Br		24.3 ± 6.7
22	H	OMe		37.5 ± 11.0
23	Cl	H		0.62 ± 0.05
24	Br	H		2.4 ± 0.5
25	OMe	H		32.8 ± 12.6
26	H	OH		25.6 ± 6.9
27	OH	H		0.10 ± 0.03

IC_{50} of 0.10 ± 0.03 μg/mL. Replacement of 4-hydroxyl group with chloro, bromo or methoxy group resulted in 6- to 300-fold loss of activity (**23**–**25**). In comparison with **27**, movement of the hydroxyl group to 3-position led to a significant decrease in inhibitory activity (**26**), while a further decrease was not observed in isosteric replacement of the hydroxyl group with chloro, bromo, or methxoy group at 3-position (**20**–**22**). In the case of compounds (**15**–**19**) with two substituents at 3,4-positons, both introduction of electron-donating group (methoxy) and electron-withdrawing group (chloro and fluoro) led to complete loss in activity, indicating that these substituents may cause a steric clash with the protein.

2.4. Antibacterial activity

Compounds with IC_{50} <30 μM against *S. aureus* TyrRS were tested against representative Gram-positive organisms (*Bacillus subtilis* ATCC 6633, *S. aureus* ATCC 25923, *Candica albicans* ATCC 10231) and a Gram-negative organism (*Escherichia coli* ATCC 35218), and the results are presented in Table 4. Two of the tested compounds showed good activity against Gram-positive organisms, especially against *S. aureus* and *C. albicans*, while all of them were inactive against Gram-negative bacterium, *E. coli*. Compound **23** and **27** displayed levels of inhibition against *C. albican* compared to marketed antibiotics, ketoconazole. Out of the synthetic compounds, **27** was the most active antibacterial tested against *S. aureus* with MIC_{50} of 0.23 μg/mL. From comparing the data in Table 3 and Table 4, a positive correlation between the IC_{50} values in the enzyme assay and the MIC_{50} values against whole cell bacteria was found. This suggests that the antibacterial activity of 4-alkoxy-3-arylfuran-2(5*H*)-ones, as that of 4-alkylamino-3-arylfuran-2(5*H*)-ones,[17] may be due to their inhibition against TyrRS.

2.5. Molecular docking

With the aim to explore the structural determinants responsible for the activity of these new inhibitors of TyrRS, molecular docking of the most potent inhibitor **27** into SB-239629 binding site of TyrRS was performed on the binding model based on the TyrRS complex structure (1jij.pdb).[2] The binding model of compound **27** and TyrRS is depicted in Figure 2 and the enzyme surface model was showed in Figure 3, which revealed that the molecular is well filled in the active pocket.

Several hydrogen-bonding interactions together with some hydrophobic interactions anchoring **27** to the active site tightly may explain its excellent inhibitory activity. In brief, the morpholine-ring system in the side chain of **27** occupies the SB-239629 piperidyl-binding pocket, and was oriented towards the entrance cavity (Fig. 3) surrounded by Gly38, His50, Pro53, Gly193 and Gln196. The O atom of morpholine-ring as a hydrogen bond acceptor is hydrogen-bonded to the backbone nitrogen of Gly193 with H···O bond length of 1.974 Å (Fig. 2). Obviously, the morpholine-ring system was located at a hydrophilic pocket of the active site. Thus,

Table 4
Inhibitory activity (IC_{50}) of the synthetic compounds against microbes.

Compound	MIC_{50} (μg/mL)			
	A	B	C	D
6	>50	34.3	>50	>50
11	47.4	10.4	34.2	>50
12	>50	16.5	>50	>50
21	>50	25.5	>50	>50
22	>50	40.8	>50	>50
23	8.6	1.3	2.9	>50
24	15.8	3.0	12.7	>50
26	47.4	34.3	47.2	>50
27	2.1	0.23	1.1	>50
Kanamycin	0.48	1.2	—	—
Penicillin	—	—	—	2.7
Ketoconazole	—	—	3.8	—

Note: (A) *B. subtilis* ATCC 6633; (B) *S. aureus* ATCC 25923; (C) *C. albicans* ATCC 10231; (D) *E. coli* ATCC 35218.

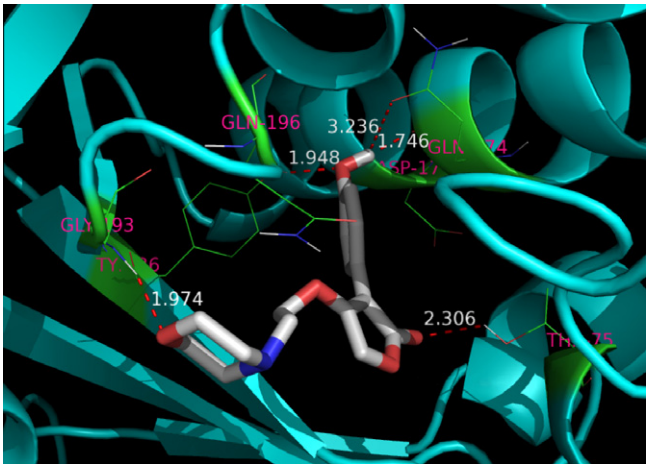

Figure. 2. Binding mode of compound **27** with TyrRS from *S. aureus*. For clarity, only interacting residues were labeled. Hydrogen bonding interactions are shown in dash. This figure was made using PyMol.

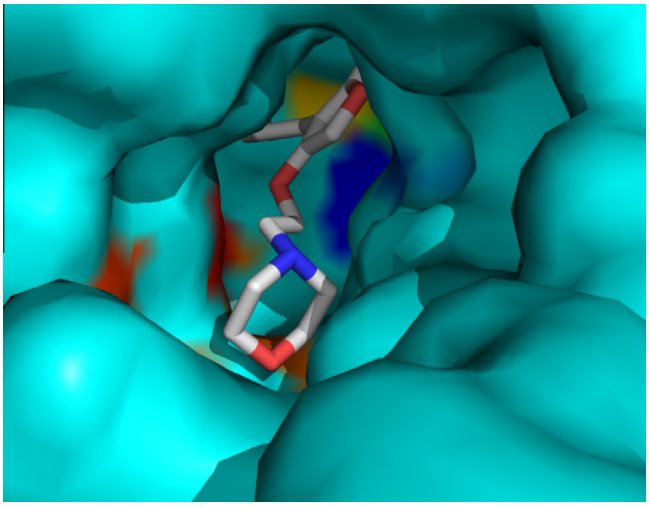

Figure 3. Binding mode of compound **27** with TyrRS. The enzyme is shown as surface; while **27** docked structures are shown as sticks. This figure was made using PyMol.

replacement of the morpholine-ring with a hydrophobic group such as piperidine-ring will significantly decrease the potency, which is consistent with the experimental data. On the contrary, replacement with a substituent containing stronger hydrophilic groups should increase the potency, and further investigations on the optimization of **27** as leading compounds are being carried out in our laboratory.

The 4-hydroxybenzene-ring moiety was located at the bottom of the active site cavity (Fig. 3), making some close interactions with Gln173 and Asp177 side chains. In addition to these interactions, three hydrogen-bonding interactions were observed: the 4-hydroxyl group as acceptor forms a O–H···O hydrogen bond with Tyr36 residue, having H···O bond length of 1.948 Å, and the 4-hydroxyl group as donor forms two O–H···O hydrogen bonds with the two carbonyl groups of Gln174 residue, having H···O bond length of 1.746 and 3.236 Å, respectively (Fig. 2). The docking model also showed that a hydrogen-bonding interaction occurs between the carbonyl group of the furanone-ring moiety and the hydroxyl group of Thr75 residue with H···O bond length of 2.306 Å. Finally, the CH_2CH_2 group linking the furanone-ring and the morpholine-ring involves a hydrophobic interaction with the CH_2CH_2 group of Gln196 residue.

Our modeling results reveal that 4-hydroxy of benzene-ring moiety and hydrophilic group substituted at the side chain are important to the interactions of the protein–ligand complex and are crucial to the potency of TyrRS inhibitory activity. Therefore, removing the hydroxyl group (or replacing with methoxy group) or substituting a hydrophobic group for the morpholine-ring (**27** vs **11** (**25**) and **11** vs **6**–**10**) obviously reduced the enzyme inhibitory activity.

3. Conclusions

In summary, we have synthesized twenty-two novel 4-alkoxy-3-arylfuran-2(5*H*)-one derivatives. Several of the target compounds showed good inhibitory activity against TyrRS from *S. aureus*, with **27** being the most active (IC_{50} = 0.10 ± 0.03 μM). Antibacterial assay revealed that the synthetic compounds are effective against growth of Gram-positive organisms (especially against *S. aureus*), while all are inactive against Gram-negative organisms. Out of the tested compounds, **27** is the most potent against *S. aureus* ATCC 25923 with MIC_{50} value (0.23 μg/mL) lower than that of the positive control (1.2 μg/mL). Molecular docking studies showed **27** well fits the active site making various close contacts with the active site residues, and disclosed that substitution of morpholine-ring in the side chain with a hydrophilic group is more suitable for further modification.

4. Experiments

4.1. Preparation of the TyrRS and enzyme assay

S. aureus TyrRS was over-expressed in *E. coli* and purified to near homogeneity (~98% as judged by SDS–PAGE) using standard purification procedures.[2] TyrRS activity was measured by aminoacylation using modifications to previously described methods.[3] The assays were performed at 37 °C in a mixture containing (final concentrations) 100 mM Tris/Cl pH 7.9, 50 mM KC1, 16 mM $MgCl_2$, 5 mM ATP, 3 mM DTT, 4 mg/ml *E. coli* MRE600 tRNA (Roche) and 10 μM L-tyrosine (0.3 μM L-[ring-3,5-3H] tyrosine (PerkinElmer, Specific activity: 1.48–2.22 TBq/mmol), 10 μM carrier). TyrRS (0.2 nM) was preincubated with a range of inhibitor concentrations for 10 min at room temperature followed by the addition of pre-warmed mixture at 37 °C. After specific intervals, the reaction was terminated by adding aliquots of the reaction mix into ice-cold 7% trichloroacetic acid and harvesting onto 0.45 mm hydrophilic Durapore filters (Millipore Multiscreen 96-well plates) and counted by liquid scintillation. The rate of reaction in the experiments was linear with respect to protein and time with less than 50% total tRNA acylation. IC_{50}s correspond to the concentration at which half of the enzyme activity is inhibited by the compound. The results are presented in Table 3.

4.2. Antimicrobial activity

The antibacterial activities of the synthesized compounds was tested against two Gram-positive bacterial strains (*B. subtilis* ATCC 6633, *S. aureus* ATCC 25923, kanamycin as positive control) and a Gram-negative bacterial strain (*E. coli* ATCC 35218, penicillin G as positive control) using LB medium, The antifungal activities of the compounds was tested against *C. albicans* ATCC 10231 (Gram-positive, ketoconazole as positive control) using RPMI-1640 medium. The MIC_{50}s of the test compounds were determined by a colorimetric method using the dye MTT.[21] A stock solution of the synthesized compound (1000 μg/ml) in DMSO was prepared and graded quantities of the test compounds were incorporated in specified quantity of sterilized liquid medium (50% (v/v) of

DMSO in PBS). A specified quantity of the medium containing the test compound was poured into 96-well plates. Suspension of the microorganism was prepared to contain approximate 10^5 cfu/mL and applied to 96-well plates with serially diluted compounds to be tested and incubated at 37 °C for 24 h. In the case of fungi, plates were incubated at 27 °C for 48 h. 50 μL of PBS containing 2 mg of MTT/mL was added to each well. Incubation was continued at room temperature for 4–5 h. The content of each well was removed, and 100 μL of 10% sodium dodecyl sulfate containing 5% isopropanol and 1 mol/L HCl was added to extract the dye. After 12 h of incubation at room temperature, the optical density (OD) was measured with a microplate reader at 550 nm. The observed MIC_{50}s were presented in Table 4.

4.3. Protocol of docking study

The automated docking studies were carried out using AutoDock version 4.2. First, AutoGrid component of the program precalculates a three-dimensional grid of interaction energies based on the macromolecular target using the AMBER force field. A grid box of 46 × 58 × 48 Å size (*x*, *y*, *z*) with a spacing of 0.375 Å and grid maps were created representing the catalytic active target site region where the native ligand was embedded. Then automated docking studies were carried out to evaluate the binding free energy of the inhibitor within the macromolecules. The genetic algorithm with local search (GA-LS) was chosen to search for the best conformers. The parameters were set using the software ADT (AutoDockTools package, version 1.5.4) on PC which is associated with AutoDock 4.2. Default settings were used with an initial population of 50 randomly placed individuals, a maximum number of 7.5×10^6 energy evaluations, and a maximum number of 2.7×10^4 generations. A mutation rate of 0.02 and a crossover rate of 0.8 were chosen. Results differing by less than 0.5 Å in positional root-mean-square deviation (RMSD) were clustered together and the results of the most favorable free energy of binding were selected as the resultant complex structures.

4.4. Crystallographic studies

X-ray single-crystal diffraction data for compound **11** was collected on a Bruker SMART APEX CCD diffractometer at 298(2) K using MoKα radiation (λ = .71073 Å) by the ω scan mode. The program SAINT was used for integration of the diffraction profiles. The structure was solved by direct methods using the SHELXS program of the SHELXTL package and refined by full-matrix least-squares methods with SHELXL.[22] All nonhydrogen atoms of compound **11** were refined with anisotropic thermal parameters. All hydrogen atoms were generated theoretically onto the parent atoms and refined isotropically with fixed thermal factors.

4.5. Chemistry

All chemicals (reagent grade) used were purchased from Aldrich (U.S.A) and Sinopharm Chemical Reagent Co. Ltd. (China). Separation of the compounds by column chromatography was carried out with silica gel 60 (200–300 mesh ASTM, E. Merck). The quantity of silica gel used was 30–70 times the weight charged on the column. Then, the eluates were monitored using TLC. Melting points (uncorrected) were determined on a XT4 MP apparatus (Taike Corp., Beijing, China). ESI mass spectra were obtained on a Mariner System 5304 mass spectrometer, and ^{1}H NMR spectra were recorded on a Bruker DPX400 or DPX300 spectrometer at 25 °C with TMS and solvent signals allotted as internal standards. Chemical shifts were reported in ppm (δ). Elemental analyses were performed on a CHN-O-Rapid instrument and were within ±0.4% of the theoretical values.

4.5.1. General procedure for preparation of compounds 1a–1m

An appropriately substituted penylacetic acid (50 mmol) was added to a solution of sodium ethoxide (60 mmol) in ethanol (70 mL) and the mixture was stirred at 25 °C for 10 min. Ethyl bromoacetate (55 mmol) was added and the stirred mixture was heated under reflux temperature for 4–6 h. The precipitated salt was filtered off and the filtrate concentrated under reduced pressure. The resulted oil was dissolved in EtOAc and washed with water and brine. Then the solution was dried over $MgSO_4$ and concentrated under reduced pressure. The oily residue was then purified by column chromatography on silica gel to give **1a**–**1m** in yields of 75–88%.

4.5.2. General procedure for preparation of compounds 2a–2m

A dropwise solution of compound **1** (10 mmol) in dry THF (10 mL) was added to a suspension of NaH (24 mmol) in dry THF (20 mL) in an ice cold bath and the stirring was maintained at room temperature for several hours (monitored by TLC). Water (30 mL) was added and the solution was extracted twice with ethyl ether. The aqueous phase was cooled to 0 °C and then acidified with concentrated hydrochloric acid to give a solid precipitate. Filtration and washing with water furnished compounds **2**. This material was used without further purification.

4.5.3. General procedure for preparation of compounds 3a–3m

Compound **2** (5 mmol) was dissolved in 35 mL of dry acetone, followed by addition of 1,2-dibromoethane (4.3 mL, 50 mmol) and triethylamine (2.2 mL, 15 mmol). The resulted mixture was refluxed for 3–5 h. After the solvent was removed, the residue was partitioned between EtOAc and water. The organic layer was then dryed over $MgSO_4$ and concentrated under reduced pressure. Flash chromatography (EtOAc/petroleum ether, from 3/2 to 2/3) furnished **3** in good yield.

4.5.4. General procedure for preparation of 4-alkoxy-3-arylfuran-2(5*H*)-ones (6–25, 4k–4m)

A mixture of compound **3** (0.5 mmol) and triethylamine (225 μL, 1.5 mmol) was dissolved in 15 mL of dry DMF and heated to 50 °C. The solution was received 3–4 interval injections of an appropriate amine (0.6 mmol) within 2 h. The mixture was then stirred for 6–10 h. After 30 mL of water was added, the resulted mixture was extracted thrice with EtOAc. The combined organic layer washed with brine and dried over $MgSO_4$. Removement of the solvent under reduced pressure gave a brown oil, which was purified by column chromatography on silica gel, eluting with $CHCl_3/CH_3OH$ (saturated with ammonia, from 37/1 to 80/1).

4.5.4.1. 3-Phenyl-4-(2-(propylamino)ethoxy)furan-2(5*H*)-one (6). White powder, 58%, mp 102–104 °C, ^{1}H NMR ($CDCl_3$): 0.57 (t, *J* = 7.3 Hz, 3H); 0.98 (t, *J* = 7.5 Hz, 1H); 1.34–1.46 (m, 2H); 3.02–3.15 (m, 2H); 3.23 (t, *J* = 5.5 Hz, 2H); 3.59 (t, *J* = 5.5 Hz, 2H); 4.86 (s, 2H); 7.24–7.37 (m, 5H); EIMS *m/z* 261 (M^+). Anal. Calcd for $C_{15}H_{19}NO_3$: C, 68.94; H, 7.33; N, 5.36. Found: C, 67.63; H, 7.32; N, 5.35.

4.5.4.2. 4-(2-(Butylamino)ethoxy)-3-phenylfuran-2(5*H*)-one (7). White powder, 43%, mp 89–91 °C, ^{1}H NMR ($CDCl_3$): 0.73 (t, *J* = 7.0 Hz, 3H); 0.81–0.99 (m, 2H); 1.28–1.42 (m, 2H); 2.32 (b s, 1H); 3.09 (t, *J* = 7.7 Hz, 2H); 3.22 (t, *J* = 5.5 Hz, 2H); 3.59 (t, *J* = 5.5 Hz, 2H); 4.85 (s, 2H); 7.26–7.36 (m, 5H); EIMS *m/z* 275 (M^+). Anal. Calcd for $C_{16}H_{21}NO_3$: C, 69.79; H, 7.69; N, 5.09. Found: C, 69.01; H, 7.68; N, 5.10.

4.5.4.3. 4-(2-(Cyclohexylamino)ethoxy)-3-phenylfuran-2(5*H*)-one (8). White powder, 54%, mp 150–152 °C, ^{1}H NMR ($CDCl_3$): 0.81–0.99 (m, 3H); 1.25–1.40 (m, 3H); 1.65–1.77 (m, 4H); 3.22 (t, *J* = 6.4 Hz, 2H); 3.27–3.35 (m, 1H); 3.48 (t, *J* = 6.3 Hz,

2H); 4.87 (s, 2H); 7.27–7.42 (m, 5H); EIMS *m/z* 301 (M^+). Anal. Calcd for $C_{18}H_{23}NO_3$: C, 71.73; H, 7.69; N, 4.65. Found: C, 72.45; H, 7.67; N, 4.66.

4.5.4.4. 3-Phenyl-4-(2-(piperidin-1-yl)ethoxy)furan-2(5*H*)-one (9). Light yellow oil, 54%, ^{1}H NMR ($CDCl_3$): 1.40–1.50 (m, 2H); 1.51–1.68 (m, 4H); 2.40–2.49 (m, 4H); 2.72 (t, *J* = 5.7 Hz, 2H); 4.22 (t, *J* = 5.5 Hz, 2H); 4.88 (s, 2H); 7.29 (d, *J* = 7.4 Hz, 1H); 7.38 (t, *J* = 7.1 Hz, 2H); 7.86 (dd, *J* = 8.6 Hz, *J* = 1.4 Hz, 2H); EIMS *m/z* 287 (M^+). Anal. Calcd for $C_{17}H_{21}NO_3$: C, 71.06; H, 7.37; N, 4.87. Found: C, 71.82; H, 7.35; N, 4.86.

4.5.4.5. 3-Phenyl-4-(2-(pyrrolidin-1-yl)ethoxy)furan-2(5*H*)-one (10). Colorless crystal, 75%, mp 81–82 °C, ^{1}H NMR ($CDCl_3$): 1.77–1.86 (m, 4H); 2.51–2.63 (m, 4H); 2.90 (t, *J* = 5.9 Hz, 2H); 4.23 (t, *J* = 5.9 Hz, 2H); 4.87 (s, 2H); 7.30 (d, *J* = 6.3 Hz, 1H); 7.38 (t, *J* = 7.1 Hz, 2H); 7.84 (d, *J* = 7.1 Hz, 2H); EIMS *m/z* 273 (M^+). Anal. Calcd for $C_{16}H_{19}NO_3$: C, 70.31; H, 7.01; N, 5.12. Found: C, 70.40; H, 6.99; N, 5.11.

4.5.4.6. 4-(2-Morpholinoethoxy)-3-phenylfuran-2(5*H*)-one (11). Colorless crystal, 63%, mp 118–119 °C, ^{1}H NMR (DMSO-d_6): 2.48 (t, *J* = 5.3 Hz, 4H); 2.74 (t, *J* = 5.5 Hz, 2H); 3.58 (t, *J* = 5.3 Hz, 4H); 4.37 (t, *J* = 5.5 Hz, 2H); 5.15 (s, 2H); 7.27 (d, *J* = 8.3 Hz, 1H); 7.39 (t, *J* = 8.3 Hz, 2H); 7.88 (d, *J* = 8.3 Hz, 2H); EIMS *m/z* 289 (M^+). Anal. Calcd for $C_{16}H_{19}NO_4$: C, 66.42; H, 6.62; N, 4.84. Found: C, 66.33; H, 6.64; N, 4.83.

4.5.4.7. 4-(2-(4-Methylpiperazin-1-yl)ethoxy)-3-phenylfuran-2(5*H*)-one (12). Colorless crystal, 85%, mp 45–46 °C, ^{1}H NMR ($CDCl_3$): 2.30 (s, 3H); 2.40–2.49 (m, 4H); 2.51–2.63 (m, 4H); 2.78 (t, *J* = 5.5 Hz, 2H); 4.22 (t, *J* = 5.5 Hz, 2H); 4.87 (s, 2H); 7.30 (d, *J* = 7.3 Hz, 1H); 7.38 (t, *J* = 7.1 Hz, 2H); 7.84 (dd, *J* = 8.0 Hz, *J* = 1.5 Hz, 2H); EIMS *m/z* 302 (M^+). Anal. Calcd for $C_{17}H_{22}N_2O_3$: C, 67.53; H, 7.33; N, 9.26. Found: C, 67.46; H, 7.32; N, 9.28.

4.5.4.8. 4-(2-(Benzylamino)ethoxy)-3-phenylfuran-2(5*H*)-one (13). Colorless crystal, 37%, mp 110–112 °C, ^{1}H NMR ($CDCl_3$): 3.27 (t, *J* = 5.3 Hz, 2H); 3.59 (t, *J* = 5.3 Hz, 2H); 4.41 (s, 2H); 4.91 (s, 2H); 7.06 (d, *J* = 6.4 Hz, 2H); 7.20–7.35 (m, 8H); EIMS *m/z* 309 (M^+). Anal. Calcd for $C_{19}H_{19}NO_3$: C, 73.77; H, 6.19; N, 4.53. Found: C, 73.84; H, 6.17; N, 4.54.

4.5.4.9. 4-(2-(2-(4-Nitrophenyl)hydrazinyl)ethoxy)-3-phenylfuran-2(5*H*)-one (14). Yellow crystal, 78%, mp 259–261 °C, ^{1}H NMR (DMSO-d_6): 3.89 (t, *J* = 5.5 Hz, 2H); 4.60 (t, *J* = 5.3 Hz, 2H); 5.16 (s, 2H); 7.28 (t, *J* = 7.5 Hz, 1H); 7.41 (t, *J* = 7.7 Hz, 2H); 7.91 (dd, *J* = 8.4 Hz, *J* = 1.3 Hz, 2H); 8.10 (d, *J* = 9.0 Hz, 2H); 8.26 (d, *J* = 8.9 Hz, 2H); EIMS *m/z* 355 (M^+). Anal. Calcd for $C_{18}H_{17}N_3O_5$: C, 60.84; H, 4.82; N, 11.83. Found: C, 60.89; H, 4.81; N, 11.84.

4.5.4.10. 4-(2-(Cyclohexylamino)ethoxy)-3-(3,4-dimethoxyphenyl)furan-2(5*H*)-one (15). Colorless crystal, 68%, mp 137–139 °C, ^{1}H NMR ($CDCl_3$): 0.80–1.02 (m, 3H); 1.23–1.42 (m, 3H); 1.60–1.74 (m, 4H); 1.93 (b s, 1H); 3.23 (t, *J* = 6.4 Hz, 2H); 3.32–3.43 (m, 1H); 3.54 (t, *J* = 6.3 Hz, 2H); 3.85 (s, 3H); 3.89 (s, 3H); 4.88 (s, 2H); 6.80 (d, *J* = 1.8 Hz, 1H); 6.81 (dd, *J* = 8.0 Hz, *J* = 1.8 Hz, 1H); 6.86 (d, *J* = 8.3 Hz, 1H); EIMS *m/z* 361 (M^+). Anal. Calcd for $C_{20}H_{27}NO_5$: C, 66.46; H, 7.53; N, 3.88. Found: C, 66.51; H, 7.51; N, 3.87.

4.5.4.11. 3-(3,4-Dimethoxyphenyl)-4-(2-(piperidin-1-yl)ethoxy)furan-2(5*H*)-one (16). Colorless crystal, 89%, mp 116–117 °C, ^{1}H NMR ($CDCl_3$): 1.38–1.49 (m, 2H); 1.51–1.67 (m, 4H); 2.46 (t, *J* = 5.0 Hz, 4H); 2.73 (t, *J* = 5.5 Hz, 2H); 3.90 (s, 3H); 3.91 (s, 3H); 4.22 (t, *J* = 5.5 Hz, 2H); 4.87 (s, 2H); 6.89 (d, *J* = 8.4 Hz, 1H); 7.50 (dd, *J* = 8.4 Hz, *J* = 2.0 Hz, 1H); 7.54 (d, *J* = 1.8 Hz, 1H); EIMS *m/z* 347 (M^+). Anal. Calcd for $C_{19}H_{25}NO_5$: C, 65.69; H, 7.25; N, 4.03. Found: C, 65.60; H, 7.27; N, 4.04.

4.5.4.12. 3-(3,4-Dimethoxyphenyl)-4-(2-(4-methylpiperazin-1-yl)ethoxy)furan-2(5*H*)-one (17). Colorless crystal, 64%, mp 69–71 °C, ^{1}H NMR (DMSO-d_6): 2.16 (s, 3H); 2.23–2.38 (m, 4H); 2.42–2.55 (m, 4H); 2.73 (t, *J* = 5.3 Hz, 2H); 3.75 (s, 3H); 3.76 (s, 3H); 4.34 (t, *J* = 5.4 Hz, 2H); 5.11 (s, 2H); 6.97 (d, *J* = 8.4 Hz, 1H); 7.49 (d, *J* = 2.0 Hz, 1H); 7.53 (dd, *J* = 8.4 Hz, *J* = 2.0 Hz, 1H); EIMS *m/z* 362 (M^+). Anal. Calcd for $C_{19}H_{26}N_2O_5$: C, 62.97; H, 7.23; N, 7.73. Found: C, 62.88; H, 7.25; N, 7.74.

4.5.4.13. 3-(3,4-Dichlorophenyl)-4-(2-(4-methylpiperazin-1-yl)ethoxy)furan-2(5*H*)-one (18). White powder, 65%, mp 92–94 °C, ^{1}H NMR (DMSO-d_6): 2.15 (s, 3H); 2.23–2.37 (m, 4H); 2.41–2.53 (m, 4H); 2.74 (t, *J* = 5.3 Hz, 2H); 4.34 (t, *J* = 5.4 Hz, 2H); 5.10 (s, 2H); 7.18 (d, *J* = 8.0 Hz, 1H); 7.28 (s, 1H); 7.43 (d, *J* = 8.1 Hz, 1H); EIMS *m/z* 370 (M^+). Anal. Calcd for $C_{17}H_{20}Cl_2N_2O_3$: C, 55.00; H, 5.43; Cl, 19.10; N, 7.55. Found: C, 55.09; H, 5.43; Cl, 19.07; N, 7.54.

4.5.4.14. 3-(3,4-Difluorophenyl)-4-(2-(piperidin-1-yl)ethoxy)furan-2(5*H*)-one (19). White powder, 43%, mp 119–121 °C, ^{1}H NMR ($CDCl_3$): 1.39–1.50 (m, 2H); 1.52–1.67 (m, 4H); 2.47 (t, *J* = 5.0 Hz, 4H); 2.75 (t, *J* = 5.4 Hz, 2H); 4.24 (t, *J* = 5.5 Hz, 2H); 4.89 (s, 2H); 7.32 (d, *J* = 8.8 Hz, 1H); 7.58 (d, *J* = 8.7 Hz, 1H); 7.65 (t, *J* = 8.8 Hz, 1H); EIMS *m/z* 323 (M^+). Anal. Calcd for $C_{17}H_{19}F_2NO_3$: C, 63.15; H, 5.92; F, 11.75; N, 4.33. Found: C, 63.07; H, 5.93; F, 11.77; N, 4.33.

4.5.4.15. 3-(3-Chlorophenyl)-4-(2-morpholinoethoxy)furan-2(5*H*)-one (20). Colorless crystal, 63%, mp 131–133 °C, ^{1}H NMR (DMSO-d_6): 2.48 (t, *J* = 5.3 Hz, 4H); 2.75 (t, *J* = 5.5 Hz, 2H); 3.57 (t, *J* = 5.3 Hz, 4H); 4.37 (t, *J* = 5.5 Hz, 2H); 5.15 (s, 2H); 7.10–7.22 (m, 3H); 7.26 (d, *J* = 8.5 Hz, 1H); EIMS *m/z* 323 (M^+). Anal. Calcd for $C_{16}H_{18}ClNO_4$: C, 59.35; H, 5.60; Cl, 10.95; N, 4.33. Found: C, 59.42; H, 5.59; Cl, 10.93; N, 4.33.

4.5.4.16. 3-(3-Bromophenyl)-4-(2-morpholinoethoxy)furan-2(5*H*)-one (21). Colorless crystal, 54%, mp 136–138 °C, ^{1}H NMR (DMSO-d_6): 2.48 (t, *J* = 5.4 Hz, 4H); 2.75 (t, *J* = 5.5 Hz, 2H); 3.58 (t, *J* = 5.3 Hz, 4H); 4.39 (t, *J* = 5.5 Hz, 2H); 5.15 (s, 2H); 7.22 (t, *J* = 8.4 Hz, 1H); 7.33 (d, *J* = 8.4 Hz, 1H); 7.37 (d, *J* = 8.2 Hz, 1H); 7.44 (s, 1H); EIMS *m/z* 367 (M^+). Anal. Calcd for $C_{16}H_{18}BrNO_4$: C, 52.19; H, 4.93; Br, 21.70; N, 3.80. Found: C, 52.25; H, 4.94; Br, 21.68; N, 3.79.

4.5.4.17. 3-(3-Methoxyphenyl)-4-(2-morpholinoethoxy)furan-2(5*H*)-one (22). Colorless crystal, 63%, mp 125–126 °C, ^{1}H NMR (DMSO-d_6): 2.48 (t, *J* = 5.4 Hz, 4H); 2.74 (t, *J* = 5.5 Hz, 2H); 3.58 (t, *J* = 5.3 Hz, 4H); 3.71 (s, 3H); 4.37 (t, *J* = 5.5 Hz, 2H); 5.15 (s, 2H); 7.12–7.24 (m, 3H); 7.26 (d, *J* = 8.5 Hz, 1H); EIMS *m/z* 319 (M^+). Anal. Calcd for $C_{17}H_{21}NO_5$: C, 46.98; H, 2.71; Br, 39.07; N, 3.42. Found: C, 46.91; H, 2.71; Br, 39.12; N, 3.42.

4.5.4.18. 3-(4-Chlorophenyl)-4-(2-morpholinoethoxy)furan-2(5*H*)-one (23). White powder, 51%, mp 124–126 °C, ^{1}H NMR (DMSO-d_6): 2.48 (t, *J* = 5.3 Hz, 4H); 2.74 (t, *J* = 5.5 Hz, 2H); 3.58 (t, *J* = 5.3 Hz, 4H); 4.38 (t, *J* = 5.5 Hz, 2H); 5.15 (s, 2H); 7.50 (d, *J* = 8.5 Hz, 2H); 7.59 (d, *J* = 8.5 Hz, 2H); EIMS *m/z* 323 (M^+). Anal. Calcd for $C_{16}H_{18}ClNO_4$: C, 59.35; H, 5.60; Cl, 10.95; N, 4.33. Found: C, 59.43; H, 5.59; Cl, 10.93; N, 4.34.

4.5.4.19. 3-(4-Bromophenyl)-4-(2-morpholinoethoxy)furan-2(5*H*)-one (24). Colorless oil, 67%, ^{1}H NMR (DMSO-d_6): 2.48 (t, *J* = 5.3 Hz, 4H); 2.75 (t, *J* = 5.5 Hz, 2H); 3.58 (t, *J* = 5.4 Hz, 4H);

4.39 (t, J = 5.5 Hz, 2H); 5.15 (s, 2H); 7.60 (d, J = 8.5 Hz, 2H); 7.87 (d, J = 8.5 Hz, 2H); EIMS m/z 367 (M^+). Anal. Calcd for $C_{16}H_{18}BrNO_4$: C, 52.19; H, 4.93; Br, 21.70; N, 3.80. Found: C, 52.26; H, 4.94; Br, 21.68; N, 3.79.

4.5.4.20. 3-(4-Methoxyphenyl)-4-(2-morpholinoethoxy)furan-2(5*H*)-one (25). Colorless crystal, 67%, mp 120–121 °C, ^{1}H NMR (DMSO-d_6): 2.48 (t, J = 5.4 Hz, 4H); 2.75 (t, J = 5.5 Hz, 2H); 3.58 (t, J = 5.4 Hz, 4H); 4.37 (t, J = 5.5 Hz, 2H); 5.15 (s, 2H); 7.43 (d, J = 8.5 Hz, 2H); 7.52 (d, J = 8.5 Hz, 2H); EIMS m/z 319 (M^+). Anal. Calcd for $C_{17}H_{21}NO_5$: C, 63.94; H, 6.63; N, 4.39. Found: C, 63.87; H, 6.65; N, 4.38.

4.5.4.21. 3-(3-(Benzyloxy)phenyl)-4-(2-morpholinoethoxy)furan-2(5*H*)-one (4k). White powder, 53%, mp 147–149 °C, ^{1}H NMR ($CDCl_3$): 2.51 (t, J = 5.3 Hz, 4H); 2.78 (t, J = 5.5 Hz, 2H); 3.60 (t, J = 5.4 Hz, 4H); 4.23 (t, J = 5.5 Hz, 2H); 4.34 (s, 2H); 5.15 (s, 2H); 7.10–7.21 (m, 3H); 7.23–7.34 (m, 5H); 7.25 (d, J = 8.5 Hz, 1H); EIMS m/z 395 (M^+). Anal. Calcd for $C_{23}H_{25}NO_5$: C, 69.86; H, 6.37; N, 3.54. Found: C, 69.77; H, 6.38; N, 3.55.

4.5.4.22. 3-(4-(Benzyloxy)phenyl)-4-(2-morpholinoethoxy)furan-2(5*H*)-one (4m). White powder, 58%, mp 143–145 °C, ^{1}H NMR ($CDCl_3$): 2.52 (t, J = 5.3 Hz, 4H); 2.78 (t, J = 5.5 Hz, 2H); 3.61 (t, J = 5.3 Hz, 4H); 4.22 (t, J = 5.5 Hz, 2H); 4.35 (s, 2H); 5.15 (s, 2H); 7.23 (d, J = 8.6 Hz, 2H); 7.24–7.35 (m, 5H); 7.55 (d, J = 8.6 Hz, 2H); EIMS m/z 395 (M^+). Anal. Calcd for $C_{23}H_{25}NO_5$: C, 69.86; H, 6.37; N, 3.54. Found: C, 69.70; H, 6.38; N, 3.54.

4.5.5. The synthesis of 26 and 27

Under a hydrogen atmosphere, Pd/C (10%, 0.30 g) was added to **4k** or **4m** (1.5 mmol) dissolved in THF/EtOH (5/15 mL). The reaction mixture was stired for 5–7 h at room temperature. After filtration of the catalyst and evaporation of the solvent, crystallization from acetone–petroleum ether produced **26** or **27**.

4.5.5.1. 3-(3-Hydroxyphenyl)-4-(2-morpholinoethoxy)furan-2(5*H*)-one (26). Colorless crystal, 88%, mp 151–152 °C, ^{1}H NMR ($CDCl_3$): 2.52 (t, J = 5.4 Hz, 4H); 2.78 (t, J = 5.5 Hz, 2H); 3.62 (t, J = 5.3 Hz, 4H); 4.22 (t, J = 5.5 Hz, 2H); 5.14 (s, 2H); 6.23 (s, 1H); 7.08–7.19 (m, 3H); 7.23 (d, J = 8.5 Hz, 1H); EIMS m/z 305 (M^+). Anal. Calcd for $C_{16}H_{19}NO_5$: C, 62.94; H, 6.27; N, 4.59. Found: C, 62.87; H, 6.26; N, 4.60.

4.5.5.2. 3-(4-Hydroxyphenyl)-4-(2-morpholinoethoxy)furan-2(5*H*)-one (27). Colorless crystal, 91%, mp 146–148 °C, ^{1}H NMR ($CDCl_3$): 2.53 (t, J = 5.3 Hz, 4H); 2.77 (t, J = 5.5 Hz, 2H); 3.60 (t, J = 5.3 Hz, 4H); 4.22 (t, J = 5.5 Hz, 2H); 5.15 (s, 2H); 6.14 (s, 1H); 7.07 (d, J = 8.6 Hz, 2H); 7.56 (d, J = 8.6 Hz, 2H); EIMS m/z 305 (M^+). Anal. Calcd for $C_{16}H_{19}NO_5$: C, 62.94; H, 6.27; N, 4.59. Found: C, 63.02; H, 6.26; N, 4.58.

Acknowledgments

The work was financed by Scientific Research Fund of Hunan Provincial Education Department (Project 09B083) of China, and by a grant (Project JSDXKYZZ0801) from Jishou University for talent introduction, China, and by Key Laboratory of Hunan Forest Product and Chemical Industry Engineering (Project JDZ201102) of China and by aid program for Science and Technology Innovative Research Team (Chemicals of Forestry Resources and Development of Forest Products) in Higher Educational Institutions of Hunan Province.

References and notes

1. Qiu, X.; Janson, C. A.; Smith, W. W.; Green, S. M.; McDevitt, P.; Johanson, K.; Carter, P.; Hibbs, M.; Lewis, C.; Chalker, A.; Fosberry, A.; Lalonde, J.; Berge, J.; Brown, P.; Houge-Frydrych, C. S.; Jarvest, R. L. *Protein Sci.* **2001**, *10*, 2008.
2. Park, S. G.; Schimmel, P.; Kim, S. *Proc. Natl. Acad. Sci.* **2008**, *105*, 11043.
3. Van de Vijver, P.; Vondenhoff, G. H. M.; Kazakov, T. S.; Semenova, E.; Kuznedelov, K.; Metlitskaya, A.; Van Aerschot, A.; Severinov, K. *J. Bacteriol.* **2009**, *191*, 6273.
4. Farhanullah, R.; Kang, T.; Yoon, E.-J.; Choi, E.-C.; Kim, S.; Lee, J. *Eur. J. Med. Chem.* **2009**, *44*, 239.
5. Hoffmann, M.; Torchala, M. *J. Mol. Model.* **2009**, *15*, 665.
6. Balg, C.; De Mieri, M.; Huot, J. L.; Blais, S. P.; Lapointe, J.; Chênevert, R. *Bioorg. Med. Chem.* **2010**, *18*, 7868.
7. Van de Vijver, P.; Ostrowski, T.; Sproat, B.; Goebels, J.; Rutgeerts, O.; Van Aerschot, A.; Waer, M.; Herdewijn, P. *J. Med. Chem.* **2008**, *51*, 3020.
8. Van de Vijver, P.; Vondenhoff, G. H. M.; Denivelle, S.; Rozenski, J.; Verhaegen, J.; Van Aerschot, A.; Herdewijn, P. *Bioorg. Med. Chem.* **2009**, *17*, 260.
9. Weber, V.; Rubat, C.; Duroux, E.; Lartigue, C.; Madesclaire, M.; Coudert, P. *Bioorg. Med. Chem.* **2005**, *13*, 4552.
10. Black, D. K. *J. Chem. Soc.* **1966**, *23*, 1123.
11. Bailly, F.; Queffèlec, C.; Mbemba, G.; Mouscadet, J. F.; Pommery, N.; Pommery, J.; Hènichart, J. P.; Cotelle, P. *Eur. J. Med. Chem.* **2008**, *43*, 1222.
12. Lattmann, E.; Dunn, S.; Niamsanit, S.; Sattayasai, N. *Bioorg. Med. Chem. Lett.* **2005**, *15*, 919.
13. Ueki, T.; Kinoshita, T. *Org. Biomol. Chem.* **2004**, *2*, 2777.
14. Lattmann, E.; Sattayasai, N.; Schwalbe, C. S.; Niamsanit, S.; Billington, D. C. *Curr. Drug Discovery Technol.* **2006**, *3*, 125.
15. Xiao, Z.-P.; Xue, J.-Y.; Tan, S.-H.; Li, H.-Q.; Zhu, H.-L. *Bioorg. Med. Chem.* **2007**, *15*, 4212.
16. Xiao, Z.-P.; Fang, R.-Q.; Li, H.-Q.; Xue, J.-Y.; Zheng, Y.; Zhu, H.-L. *Eur. J. Med. Chem.* **2008**, *43*, 1828.
17. Xiao, Z.-P.; He, X.-B.; Peng, Z.-Y.; Xiong, T.-J.; Peng, J.; Chen, L.-H.; Zhu, H.-L. *Bioorg. Med. Chem.* **2011**, *19*, 1571.
18. Xiao, Z.-P.; Zhu, J.; Jiang, W.; Li, G.-X.; Wang, X.-D. Z. *Kristallogr. NCS* **2010**, *225*, 797.
19. Fujihara, T.; Katafuchi, Y.; Iwai, T.; Terao, J.; Tsuji, Y. *J. Am. Chem. Soc.* **2010**, *132*, 2094.
20. Xiao, Z.-P.; Yan, W.-B.; Liu, Z.-X.; Chen, L.-H.; Peng, X.-C. *Acta Cryst.* **2010**, *E66*, o3068.
21. Chiou, C. C.; Mavrogiorgos, N.; Tillem, E.; Hector, R.; Walsh, T. *J. Antimicrob. Agents Ch.* **2001**, *45*, 3310.
22. Sheldrick, G. M. *SHELXTL-97, Program for Crystal Structure Solution and Refinement*; University of Göttingen: Göttingen, Germany, 1997.